THE JOURNAL OF BIOLOGICAL CHEMISTRY
Vol. 279, No. 53, Issue of December 31, pp. 55801–55808, 2004
Printed in U.S.A.

Thyroxine-Thyroid Hormone Receptor Interactions*

Received for publication, September 2, 2004
Published, JBC Papers in Press, October 4, 2004, DOI 10.1074/jbc.M410124200

Ben Sandler‡, Paul Webb§, James W. Apriletti§, B. Russell Huber‡, Marie Togashi§, Suzana T. Cunha Lima§, Sanja Juric¶, Stefan Nilsson¶, Richard Wagner‡, Robert J. Fletterick‡, and John D. Baxter§‖

From the §Metabolic Research Unit and Diabetes Center and the ‡Departments of Biochemistry and Biophysics, University of California, San Francisco, California 94122 and ¶KaroBio AB, Novum S-141 57, Huddinge, Sweden

Thyroid hormone (TH) actions are mediated by nuclear receptors (TRs α and β) that bind triiodothyronine (T_3, 3,5,3′-triiodo-L-thyronine) with high affinity, and its precursor thyroxine (T_4, 3,5,3′,5′-tetraiodo-L-thyronine) with lower affinity. T_4 contains a bulky 5′ iodine group absent from T_3. Because T_3 is buried in the core of the ligand binding domain (LBD), we have predicted that TH analogues with 5′ substituents should fit poorly into the ligand binding pocket and perhaps behave as antagonists. We therefore examined how T_4 affects TR activity and conformation. We obtained several lines of evidence (ligand dissociation kinetics, migration on hydrophobic interaction columns, and non-denaturing gels) that TR-T_4 complexes adopt a conformation that differs from TR-T_3 complexes in solution. Nonetheless, T_4 behaves as an agonist *in vitro* (in effects on coregulator and DNA binding) and in cells, when conversion to T_3 does not contribute to agonist activity. We determined x-ray crystal structures of the TRβ LBD in complex with T_3 and T_4 at 2.5-Å and 3.1-Å resolution. Comparison of the structures reveals that TRβ accommodates T_4 through subtle alterations in the loop connecting helices 11 and 12 and amino acid side chains in the pocket, which, together, enlarge a niche that permits helix 12 to pack over the 5′ iodine and complete the coactivator binding surface. While T_3 is the major active TH, our results suggest that T_4 could activate nuclear TRs at appropriate concentrations. The ability of TR to adapt to the 5′ extension should be considered in TR ligand design.

Thyroid hormone (TH)[1] plays important regulatory roles in metabolism, homeostasis, and development by binding and altering the transcriptional regulatory properties of two related nuclear receptors (NRs), the thyroid hormone receptors (TRs) α and β (1, 2). Most TH produced in the thyroid gland is secreted in the form of thyroxine (T_4; 3,5,3′,5′-tetraiodo-L-thyronine) (2, 3). The thyroid gland also produces smaller amounts of triiodothyronine (T_3; 3,5,3′-triiodo-L-thyronine) and reverse T_3 (rT_3; 3,3′,5′-triiodo-L-thyronine), and 80% of T_4 is converted to T_3 and rT_3 in peripheral tissues by two selenium deiodinases, which are tissue-specific (4). Current beliefs are that T_3 is the dominant active form of TH; T_3 binds the TRs with an affinity about 20–30 times higher than that of T_4 (5–9), and some studies suggest that T_3 is present at higher concentrations in the nucleus than T_4 (10, 11). Nonetheless, the question of whether T_4 is simply a prohormone or an active TH species is not completely resolved. T_4 exerts rapid nongenomic effects at several loci distinct from TRs (12). Moreover, saturating levels of T_4 activate transcription of TH-responsive genes in cell culture (see for example Ref. 5). Whereas it is possible that at least some of this activity is due to T_3 generated from T_4 in the cell, these results suggest that T_4 may act as a TR agonist. Normal concentrations of plasma-free T_4 are about 4–6-fold higher than those of T_3 (19 pmol/liter of T_4 *versus* 4.3 pmol/liter T_3) and intracellular T_4 and T_3 levels can differ because of variations in uptake and T_4 to T_3 conversion (3); thus, it is conceivable that intracellular T_4 in some context could occupy a significant fraction of nuclear TRs.

If T_4 does behave as an agonist, then it should bind to TR in a similar way to T_3 and induce conformational changes in the TR similar to those induced by T_3 (13, 14). T_3 interacts with the TR ligand binding domain (LBD), located in the receptor C terminus. The x-ray crystal structure of TRα or TRβ complexed with T_3 reveals that hormone is completely enclosed in a ligand binding pocket within the core of the LBD. It is thought that the enclosure is due to ligand-induced packing of the LBD C-terminal helix 12 (H12) against the LBD; a rearrangement that also disrupts the corepressor binding surface and completes the coactivator binding surface, leading to exchange of coregulators and influence on gene expression *in vivo* (15).

Unlike T_3, T_4 possesses a bulky iodine substituent at the 5′-position of the first thyronine ring. X-ray crystal structures have been determined for TR-LBDs complexed with several different high affinity agonists, including T_3, Dimit (3, 5-dimethyl-3′isopropyl-L-thyronine), and the TRβ-specific ligands GC-1 (3,5 dimethyl-4-(4-hydroxy-3′-isopropylbenzyl)-phenoxy acetic acid), and KB141 (3,5-dichloro-4-[(4-hydroxy-3-isopropylphenoxy)phenyl] acetic acid) (16–18). In each of these cases,

* This work was supported by Grants DK41842 and DK64148 (to J. D. B.) and DK58390 (to R. J. F) from the National Institutes of Health. The costs of publication of this article were defrayed in part by the payment of page charges. This article must therefore be hereby marked "*advertisement*" in accordance with 18 U.S.C. Section 1734 solely to indicate this fact.

The atomic coordinates and structure factors (codes 1YOX and 1XZX) have been deposited in the Protein Data Bank, Research Collaboratory for Structural Bioinformatics, Rutgers University, New Brunswick, NJ (http://www.rcsb.org/).

‖ Has proprietary interests in, and serves as a consultant and deputy director to Karo Bio AB, which has commercial interests in this area of research. To whom correspondence should be addressed: Metabolic Research Unit and Diabetes Center, University of California School of Medicine, HSW1210, 513, Parnassus Ave., San Francisco, CA 94122-0540. Tel.: 415-476-3166; Fax: 415-564-5813; E-mail: Jbaxter918@aol.com.

[1] The abbreviations used are: TH, thyroid hormone; LBD, ligand binding domain; TR, thyroid receptor; T_3, triiodothyronine (3,5,3′-triiodo-L-thyronine); T_4, thyroxine (3,5,3′,5′-tetraiodo-L-thyronine); R.m.s., root mean square; MIBRT, 3,5-dibromo-4-(3′isopropyl-4′-hydroxyphenoxy)benzoic acid); DIBRT, 3,5-dibromo-4-(3′,5′-diisopropyl-4′-hydroxyphenoxy)benzoic acid; HIC, hydrophobic interaction columns; Dimit, 3, 5-dimethyl-3′isopropyl-L-thyronine; NR, nuclear receptor.

the agonist contains a 5′ hydrogen group that lies close to the inner surface of H12. We therefore predicted that compounds with bulky side groups would perturb the folding of H12 against the body of the LBD and exploited this feature to create TR antagonists based on the notion that 5′ extensions would preclude appropriate H12 packing and coactivator binding (19–24). For example, addition of a 5′ isopropyl group, similar in size to an iodine group, to the agonist MIBRT (3,5-dibromo-4-(3′isopropyl-4′-hydroxyphenoxy)benzoic acid) creates the TR antagonist DIBRT (3,5-dibromo-4-(3′,5′-diisopropyl-4′-hydroxyphenoxy)benzoic acid) (22). Thus, it is conceivable that T_4, with a 5′ iodine extension, could even behave as an antagonist in some settings. Improved understanding of the way that the TRs adapt to the 5′ iodine group will be therefore important for understanding T_4 action and key principles of NR antagonist design.

In this study, we examine T_4 interactions with TR, the way that T_4 influences TR activity *in vitro* and in cells in culture and determined the x-ray crystal structure of TR in complex with T_4. We find that the TR-T_4 complex is less stable than the TR-T_3 complex, and that T_4-liganded TRs exhibit properties that are similar to unliganded TRs in solution. Nonetheless, T_4 behaves as an agonist in cell-free assays and transfected cells. The x-ray structure of the TR LBD-T_4 complex reveals that a previously undetected niche in the ligand binding pocket widens, relative to the size of the pocket observed in the TRβ-T_3 complex, to accommodate the 5′ iodine, permitting H12 to pack against the LBD surface in the presence of the larger ligand. Thus, the enclosed TR hormone binding pocket accommodates T_4 without complete disruption of overall TR-LBD structure. These results suggest that T_4 will act largely as a TR agonist if present at high enough concentrations in the nucleus.

MATERIALS AND METHODS

Thyroid Hormone Binding Assay—Thyroid hormone binding and analog competition assays were performed as previously described (9). K_d values were calculated by fitting saturation curves and competition data to the equations of Swillens (25) using the GraphPad Prism program (GraphPad Software, San Diego, CA).

Hydrophobic Interaction Chromatography of TR—TR-LBDs were expressed in *E. coli* and partially purified on phenyl-Toyopearl, TSK-DEAE, TSK-heparin, and TSK-phenyl columns without TH as described previously (9). For each analog tested, TR was incubated for 1 h with a 5-fold molar excess of the analog relative to the final TR concentration, ammonium sulfate concentration was adjusted to 0.7 M, and the sample was loaded and chromatographed on a 0.8 × 7.5 cm TSK-phenyl column (Tosoh Biosep, Montgomeryville, PA) at 0.75 ml/min with a 60-min gradient from 0.7 M ammonium sulfate, no glycerol to no salt, 20% glycerol. TR levels were assessed by measuring absorption at 280 nM and, where appropriate, radiolabeled T_4 in complex with the TR was detected by scintillation.

GST Pull-down Assay—Labeled TRs were expressed using a TnT-coupled transcription translation kit. GRIP1 (amino acids 563–1121) (26), TRAP220-(622–701) (27), and N-CoR-(1944–2453) (28) were prepared in *Escherichia coli* BL21 as a fusion protein with glutathione *S*-transferase as per the manufacturer's protocol (Amersham Biosciences). Binding experiments were performed by mixing glutathione-linked Sepharose beads containing 4 μg of GST fusion proteins (Coomassie Plus protein assay reagent, Pierce) with 1–2 μl of ^{35}S-labeled TR in 150 μl of binding buffer (20 mM HEPES, 150 mM KCl, 25 mM $MgCl_2$, 10% glycerol, 1 mM dithiothreitol, 0.2 mM phenylmethylsulfonyl fluoride, protease inhibitors, and 20 μg/ml bovine serum albumin) for 1.5 h. Beads were washed three times with 200 μl of binding buffer, and bound proteins were separated using 10% SDS-polyacrylamide gel electrophoresis and visualized by autoradiography.

Electrophoretic Mobility Shift Assays—In vitro translated TR was produced in reticulocyte lysates, TnT T7 Quick (Promega), and 20 fmols of translated receptor were incubated with 300,000 cpm of [γ-^{32}P]ATP-radiolabeled F2 oligonucleotides and 1 μg of poly(dI-dC) (Amersham Biosciences) in a 20-μl volume (29–31). The binding buffer contained 25 mM HEPES, 50 mM KCl, 1 mM dithiothreitol, 10 μM $ZnSO_4$, 0.1% Nonidet P-40, 5% glycerol. After 30 min at room temperature, the mixture was loaded onto a 5% nondenaturing polyacrylamide gel that was previously run for 30 min at 200 V. To separate TR-DNA complexes, the gel was run at 4 °C for 120–180 min at 200 V, using a running buffer containing 45 mM Tris borate (pH 8.0), and 1 mM EDTA.

Reporter Cells—The assay procedure, described previously (22), utilized Chinese hamster ovary cells stably expressing TRα1 and TRβ1 containing a stably integrated reporter gene with a single TRE (DR-4) cloned into the position of the mouse mammary tumor virus promoter hormone response element, driving expression of alkaline phosphatase coding sequences.

Crystallization and Data Collection—The TRβ LBD was purified for crystallization trials using cobalt affinity and hydrophobic interaction chromatography first without and then with hormone as previously described (18). Crystals of the T_3 complex were obtained by the hanging drop method, with a 10.5 mg/ml protein stock solution and mother liquor consisting of 100 mM sodium cacodylate and 900 mM sodium acetate, pH 7.2. Crystals were cryoprotected by immersion in sequential baths of 100 mM sodium cacodylate and 1.1 M sodium acetate, pH 7.2, with 3, 8, and 15% glycerol. Crystals were subjected to a final swipe through a bath with 25% glycerol before flash-freezing in liquid nitrogen.

Crystals of the T_4 complex were obtained similarly, with a crystallization mother liquor of 100 mM sodium cacodylate and 700 mM sodium acetate, pH 7.4. Use of extremely fresh protein and microseeding with Triac-hTRβ LBD crystals (< 0.1% of the final crystal) were found to be essential to obtaining diffraction quality crystals. Crystals were then cryoprotected using sequential glycerol baths as for the T_3 complex, but with a mother liquor of 100 mM sodium cacodylate and 900 mM sodium acetate, pH 7.4. Crystals were analyzed at the Advanced Light Source synchrotron facility, beamline 5.02. For the T_3 complex, 135° of data were collected with 1.5° oscillations; for the T_4 complex, 73° of data were collected with 0.5° oscillations. Reflections were indexed in DENZO and scaled in SCALEPACK.

Structural Refinement of the T_3 Complex—A molecular replacement solution was found using EPMR, employing the wild-type TRβ/TRIAC structure with hormone omitted as a probe. The structure was then subjected to multiple rounds of simulated annealing, followed by positional and B-factor refinement in CNS. Occupancies were refined in CNS for arsenic atoms only. Refinement was then continued using REFMAC of the CCP4 suite. In the final stages of refinement, water molecules were added to the structure both manually and in ARP/wARP. Refinement steps alternated with manual rebuilding steps in Quanta98 and O, guided by $F_o - F_c$ and $2F_o - F_c$ maps calculated using FFT of the CCP4 suite, and a simulated annealing omit map calculated using CNS.

Structural Refinement of the T_4 Complex—The T_4 data set was subjected to molecular replacement in EPMR and simulated annealing and positional, B-factor, and occupancy refinement in CNS as for the T_3 complex. In light of the markedly higher resolution of the data for the T_3 complex, the refined T_3 structure was then least squares fitted in O to the model of the T_4 complex. A composite model consisting of protein from the fitted T_3 complex and ligand from the T_4 complex was created and used for subsequent refinement against the T_4 complex data.

To guard against model bias, this composite model was subjected to simulated annealing and positional refinement in CNS. However, this treatment raised R_{free} markedly, as compared with R_{free} of the composite after positional refinement only. This indicates that the true structure of the T_4 complex is close to the T_3 complex model used to create the composite. Subsequent refinement and model rebuilding were carried out as described above for the T_3 complex.

RESULTS

The TR-T_4 Complex Is Less Stable Than the TR-T_3 Complex and Adopts a Different Conformation in Solution—We first investigated interactions of TRs with T_3 and T_4 (Fig. 1*A*). We previously determined that T_3 has an affinity for TRs (K_d = 0.06 nM) about 30-fold higher than T_4 (K_d = 2 nM) (6). T_4 also dissociates from TRs more rapidly than T_3 (Fig. 1, *B* and *C*). Whereas it took 8.4 and 6.2 h for half the T_3 to dissociate from *in vitro* translated preparations of TRα and TRβ at 4 °C, it only took about 0.15 h and 0.06 h for half of the T_4 to dissociate from TRα and TRβ, respectively. Thus, TRs form a complex with T_4 that is significantly less stable than the TR-T_3 complex.

We next examined elution of T_4-liganded TRs from TSK-

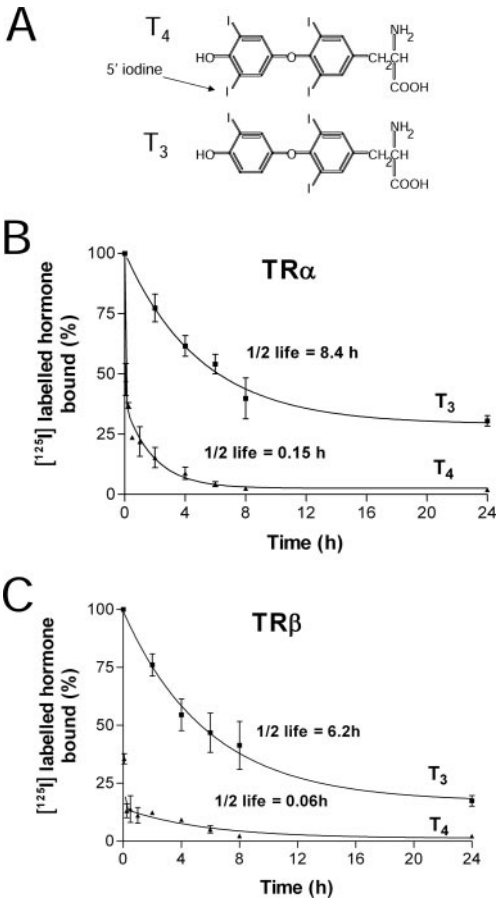

FIG. 1. **TR interactions with T_3 and T_4.** *A*, structures of T_3 and T_4 are presented with the iodine group at the 5′ position of the first thyronine ring *highlighted*. *B*, dissociation curves for T_3 and T_4 determined with the TRα LBD. *C*, as above, but determined with the TRβ-LBD.

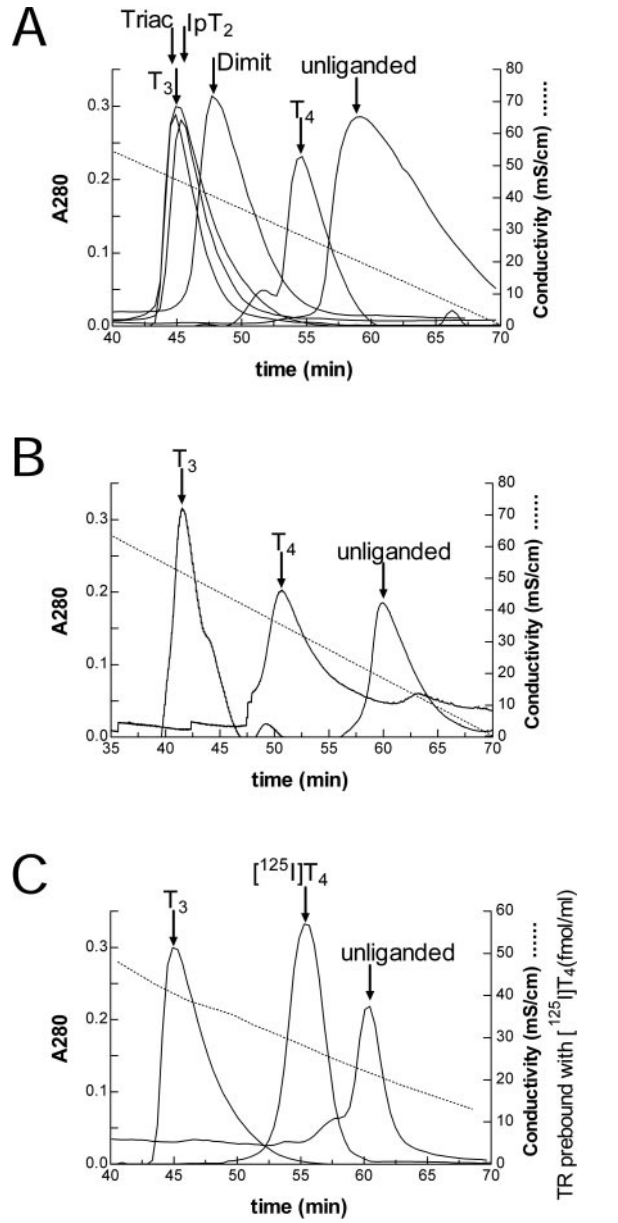

FIG. 2. **TR-T_3 and TR-T_4 complexes adopt different conformations.** *A*, elution profiles for purified TRα LBDs in complex with different agonist ligands or unliganded from hydrophobic interaction chromatography columns. *B*, as above, with TRβ LBD. *C*, as in *A*, with TRs bound to labeled T_4.

phenyl hydrophobic interaction columns (HIC), an assay that detects ligand-dependent conformational alterations in TR-LBDs and provides a crude index of hydrophobicity (9). In accordance with previous results (9), liganded TRα-LBDs eluted ahead of unliganded TRs (Fig. 2*A*). Moreover, TR preparations in complex with several agonists T_3, Triac (3,3′,5′-triiodothyroacetic acid), 3′-IpT_2 (3′-isopropyl-3,5-diiodo-L-thyronine), and Dimit eluted nearly together, with elution order paralleling relative affinities of ligand for TR (T_3 = Triac > IpT_2 > Dimit). By contrast, the TRα-T_4 complex eluted closer to unliganded TR. Similar results were also obtained with the TRβ LBD; the TRβ-T_4 complex eluted from the column between the TRβ-T_3 complex and unliganded TRβ (Fig. 2*B*).

It is unlikely that the unusual elution profile of the TR-T_4 complex is related to the low affinity of T_4 for TRs; the TRα-Dimit complex eluted at a similar position to other TR agonist complexes even though Dimit binds TRα with an affinity five times lower than T_4 (K_d = 9 nM for Dimit *versus* 2 nM for T_4). It is also unlikely that the unusual elution profile is related to rapid T_4 release during passage over HIC. Continuous dissociation of T_4 would lead to a broad curve and not a discrete symmetric peak as observed here, although the "shoulder" observed with the TRβ-T_4 complex may reflect T_4 dissociation (Fig. 2*B*). Nonetheless, we directly examined migration of [^{125}I]T_4 prebound to TRα on HIC (Fig. 2*C*). Radiolabeled T_4 migrated at the same position as the TRα-T_4 complex, whereas free T_4 did not elute from the column in these timescales (not shown), confirming that TR remains bound to T_4 as it passes over HIC. Thus, the unique elution profile of the TR-T_4 complex reflects an unusual conformation that exposes more hydrophobic surface than TRs in complex with T_3 or other analogues.

Modulator Binding Properties of TR-T_4 Complexes Resemble Those of TR-T_3 Complexes—We next determined whether T_4 behaved as an agonist under cell-free conditions. Fig. 3*A* shows that T_4 and T_3 promoted equivalent levels of TR binding to bacterially expressed nuclear receptor interacting regions of the coactivators GRIP1 and TRAP220. T_4 and T_3 also showed comparable activity in promoting binding of radiolabeled full-length GRIP1 and TRAP220 to bacterially expressed TRβ-LBD (not shown). Finally, both ligands promoted TR release from bacterially expressed preparations of the receptor-interacting region (C terminus) of the corepressor, N-CoR (Fig. 3*B*). Thus, T_4 and T_3 behave as agonists in cell-free conditions.

TR agonists promote near complete dissociation of TR dimers, but not RXR-TR heterodimers, from DNA response

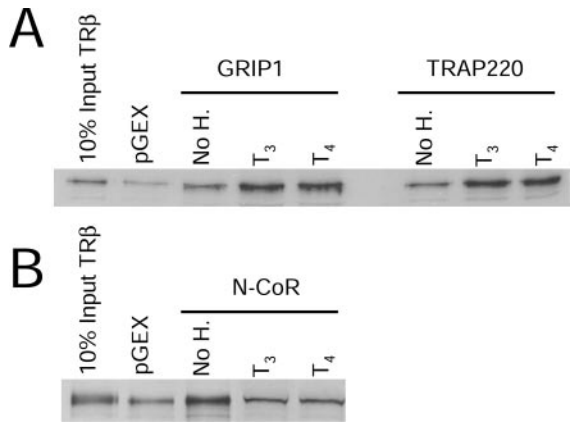

FIG. 3. **T_4 acts as an agonist *in vitro*.** *A*, autoradiograms of SDS-polyacrylamide gels, showing the amount of radiolabeled TRβ retained on columns containing bacterially expressed nuclear receptor-interacting fragments of GRIP1 and TRAP220. *B*, as in *A*, except that the NR-interacting region of the corepressor N-CoR is used as bait for TR.

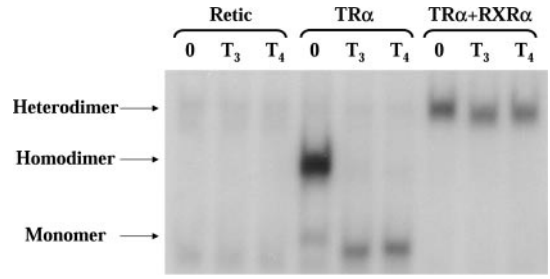

FIG. 4. **T_4 resembles T_3 in effects on TR DNA binding activities.** The figure shows an autoradiogram of an electrophoretic mobility shift assay to resolve a radiolabeled F2/IP-6 oligonucleotide in complex with hTRα or hTRα/RXRα heterodimers (±) different forms of TH.

elements (TREs) containing half-sites aligned as inverted palindrome (F2/IP-6) or direct repeats (DR-4) (29, 30). T_4 and T_3 both promoted TRα homodimer release from an F2/IP-6 element and enhanced interactions of TR monomers with the same element (Fig. 4). Both forms of TH only modestly reduced RXR-TRα heterodimer binding in the same conditions. Similar results were also obtained using DR-4, and with TRβ and both TREs (not shown). Nonetheless, TR migration was slower in the presence of T_4 than T_3 (this was most evident for the monomer). Thus, T_4 resembles T_3 in terms of regulation of DNA binding activity, but TR-T_4 and TR-T_3 complexes exhibit different mobilities, underscoring the idea that TR-T_4 complexes adopt a different structure from TR-T_3 complexes in solution (see Fig. 2).

T_4 Behaves as a TR Agonist in Cell Culture—We next examined the behavior of T_4 in cell culture. T_4 elicited a similar maximal response to T_3 in cultured chinese hamster ovary cells that were stably transfected with a TH-regulated reporter gene and a vector that expresses either TRα (TRAFα cells, Fig. 5*A*) or TRβ (TRAFβ cells, Fig. 5*B*) (22, 32). In both cases T_4 exhibited a potency that is about 10% that of T_3. It is unlikely that T_4 to T_3 conversion accounts for the activity of administered T_4 in these conditions for several reasons. Treatment of TRAF cells with optimal doses of the deiodinase inhibitors iopanoic acid or propylthiouracil (PTU) did not alter the T_3 or T_4 dose response, and we did not detect significant T_4 to T_3 conversion assayed by high performance liquid chromatography of TRAF cell extracts (not shown). Moreover, spiking T_4 preparations with T_3 (to account for 10% of total TH on a molar basis) yielded a leftward shift in EC_{50} relative to T_4 alone (Fig. 5*C*), suggesting that T_4 to T_3 conversion of 10% (and probably lower) can be detected in this system. Thus, T_4 behaves as a full agonist in cells in conditions in which conversion to T_3 is unlikely to contribute significantly to agonist activity.

The X-ray Crystal Structure of the TRβ-T_4 Complex Reveals That the LBD Adapts to the 5′-Iodine of T_4 and Completes the Coactivator Binding Surface—To determine how TRs accommodate T_4 within the ligand binding pocket and perceive the compound as an agonist despite the presence of the bulky 5′ iodine group, we obtained structures of the TRβ-LBD in complex with T_3 and T_4. Data collection and refinement statistics are presented in Table I. A ribbon diagram of the T_4-liganded TRβ structure (*pink*), superimposed over the T_3-liganded TRβ structure (*cyan*) is shown in Fig. 6. The complexes are similar in overall fold, both to each other and to previously determined structures of TR LBDs bound to agonists. Moreover, T_4 is completely buried within the core of the LBD, just like other agonists. The TRβ-T_3 structure has a pocket volume of 572 Å^3, whereas the TRβ-T_4 structure exhibits a pocket volume of 607 Å^3, as determined by GRASP (33). The TRβ-T_3 and TRβ-T_4 structures share the same space group and crystal contacts. Thus, differences in pocket volume between these two structures are probably attributable to the difference in the size of the ligand.

Direct comparisons of the TR-T_4 and TR-T_3 complexes (using "blinking" between aligned LBD structures in Insight II (Accelrys)) revealed concerted backbone shifts in four distinct regions. The first comprises H12, the H11-H12 loop and the wall of the ligand binding pocket and lies close to the 5′ iodine group (Fig. 6). The other regions include: N-terminal residues 199–212 (part of the DNA binding domain C-terminal helix (H0), which is included in this structure); H2 residues 234–243, portions of the underlying β-sheet (residues 318–321 and 325–339) and the loop between H2 and H3; and the N terminus of H3 (residues 248–267). Each of these regions of TR usually exhibits poor electron density in crystals, suggesting that they correspond to mobile regions of the protein (16–18). Thus, alterations in these regions are less likely to be significant for understanding ligand discrimination than those of H11-H12 region.

The H11-H12 loop (residues 445–453) is shifted by about 1 Å in the TR-T_4 structure relative to the TR-T_3 structure (Fig. 7), the C terminus of H11 (residues 437–444) is pulled inwards toward the pocket, accentuating a kink also present in the T_3 structure and other agonist-bound TR LBD structures, and the C-terminal end of H12 (residue 460) is pushed outwards in the presence of T_4. Despite these alterations, residues that comprise the coactivator binding surface (on H12 and the upper part of H3 and H5) adopt a structure with backbone positions identical to those seen in the TR-T_3 structure, and side chain positions nearly identical. This is consistent with the finding that T_4 promotes coactivator binding *in vitro*, and displays agonist activity *in vivo*. Nonetheless, direct comparisons in Rasmol indicate that H12 (residues 452–460) has closer contacts with the main body of the LBD in the T_3 complex than in the T_4 complex. This suggests that H12 packs less tightly against the LBD. Moreover, the average B-factor for protein atoms was higher for TR-T_4 (54.05) than for TR-T_3 (49.61), and the TR-T_4 structure had lower resolution (3.1 Å) than the TR-T_3 structure (2.5 Å). Thus, the TRβ-T_4 complex exhibits a greater degree of disorder than the TR-T_3 structure.

The conformational alterations that occur within the hormone binding pocket near the T_4 5′ iodine group are shown in detail in Figs. 8 and 9. Strikingly, the 5′ iodine fits neatly into a small "niche" in the wall of the pocket (Fig. 8*A*). This feature is analogous to similar niches that accommodate the other iodine groups in the T_4 and T_3 structures and is comprised of two distinct parts: an upper region that consists of residues

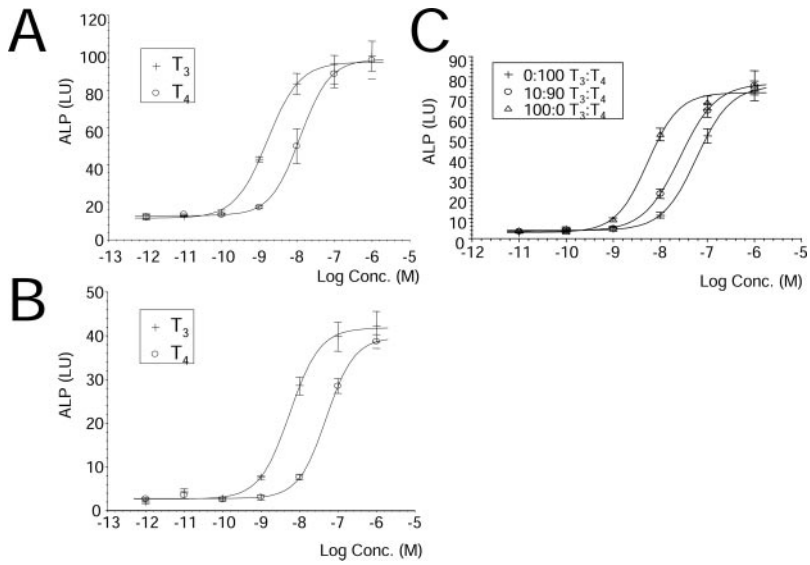

FIG. 5. **T_4 acts as an agonist in mammalian cell cultures.** *A*, graph shows alkaline phosphatase activity (the alkaline phosphatase gene is under control of a TH-regulated promoter) as a function TH concentration in chinese hamster ovary cells stably transfected with human TRα (TRAF-α cells). *B*, as in *A*, except that the experiment was performed in CHO cells stably transfected with TRβ (TRAF-β cells). *C*, as in *A*, except that an additional treatment (T_4 preparations spiked with 10% T_3) was employed.

TABLE I
Data collection and refinement statistics

	T_3	T_4
Data Collection		
Spacegroup	P3121	P3121
Cell dimensions		
a, *b* (Å)	68.764	68.790
c (Å)	130.943	130.400
Resolution (Å)	2.5	3.1
Reflections	109,848	27,682
Unique Reflections	12,903	6,881
Completeness	99.7%	99.4%
R_{sym} (overall)	0.08	0.07
R_{sym} (highest resolution shell)	0.35	0.31
Refinement		
$R_{working}$	18.38	21.96
R_{free}	24.32	26.12
R.m.s. bond length (Å)	0.031	0.040
R.m.s. bond angle (°)	2.310	2.780

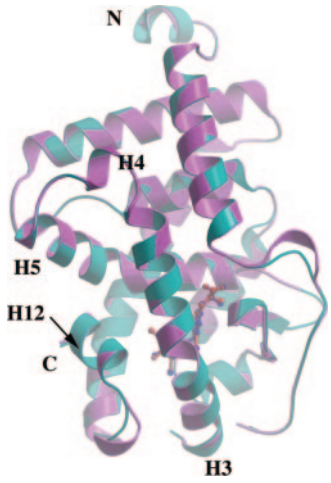

FIG. 6. **Structure of the TRβ-T_4 complex.** Superimposed ribbon diagrams of TRβ-T_3 complex (*cyan*) and the TRβ-T_4 complex (*pink*) show that the overall fold is nearly identical. The coactivator binding surface H3, 4, 5, and 12 is labeled.

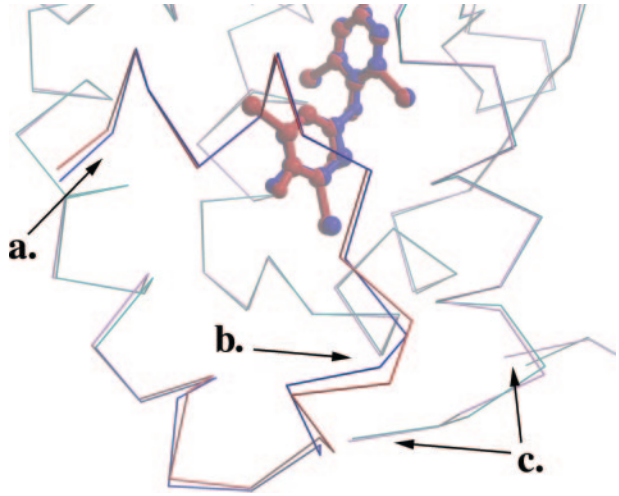

FIG. 7. **Superimposed views of the backbone trace of the TRβ H11-H12 region derived from TRβ-T_4 and TRβ-T_3 structures.** Backbone displacements in TR-T_4 (*red*) relative to TR-T_3 (*blue*). Helix 12 is *highlighted*. Displacements near the ligand binding pocket are confined to three areas: (*a*) C terminus of helix 12, (*b*) loop connecting helices 11 and 12, (*c*) disordered loop consisting of residues 250–265 linking nearby helices 2 and 3. Despite these structural alterations, the center of helix 12 shows no backbone displacement and completes the coactivator binding surface.

from several static helices that line the pocket of the LBD (Ile^{276} on H3, and Met^{310}, Met^{313} on H6), and a lower region comprised of His^{435} on H11, and Phe^{455} and Phe^{459} on H12. This precisely positioned niche permits TR to accommodate T_4 completely within the enclosed pocket despite the presence of the 5′ iodine group. The niche is also present within the TRβ-T_3 structure, but it is smaller (Fig. 8*B*). Superimposition of the TR-T_4 and TR-T_3 complexes reveals this region of the pocket expands slightly in the presence of T_4 (Fig. 9, compare *mesh surface*, T_4 with *solid surface*, T_3). This expansion is a result of a number of amino acid side chain shifts. The largest involves Met^{310} (on H6), which lies above the 5′ iodine in the TR-T_4 complex. If one considers the receptor in the orientation seen in Fig. 9, a steric clash between Met^{310} and the 5′-iodine shifts the entire ligand toward the "left" of the receptor relative to the position of ligand in the TRβ-T_3 complex (detailed in Table II). This repositioning accentuates further steric clashes between the 5′ iodine group and side chains of two residues (Phe^{455}, Phe^{459}) on H12 itself. In addition, the kink in H11 probably results from a steric clash between the 5′ iodine and His^{435} (see Table II for distances). These alterations enlarge the niche that accommodates the 5′ iodine substituent and permit H12 to pack against the LBD and complete the coactivator binding surface.

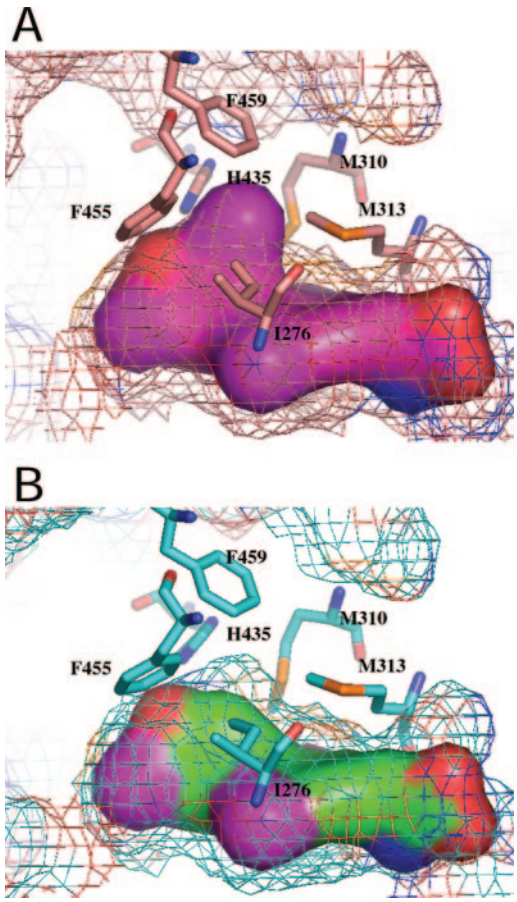

FIG. 8. **Comparison of the architecture of the TR ligand binding pocket in the presence of different ligands.** *A* and *B*, close-up view of the ligand binding pocket with side chains of the residues lining the niche, which accommodates the 5′ iodine group. Inner surfaces of the pockets are shown as *mesh contours*, whereas surfaces of the ligands are shown as *solid contours*. *A*, pocket of the TR-T_4 complex. *B*, pocket of the TR-T_3 complex. The figures were created in PyMol (pymol.sourceforge.net/).

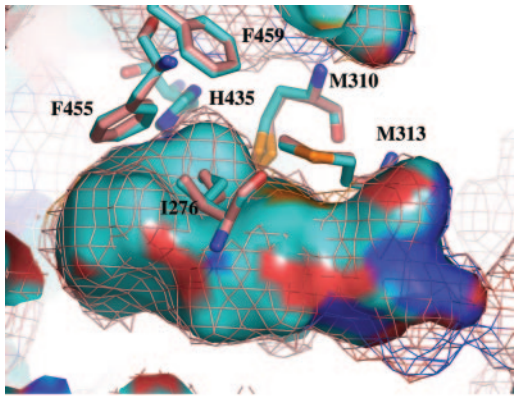

FIG. 9. **Structural alterations in the ligand binding pocket that permit TRβ to accommodate T_4.** Superimposed images of the side chains and pockets of T_4 (*pink bonds*, *mesh surface*)- and T_3- (*cyan bonds*, *solid surface*) liganded TRs.

DISCUSSION

The current studies address T_4 interactions with TRs. As developed in the Introduction, T_3 is thought to be the major active form of TH and binds TRs with ~30-fold the affinity of T_4 (6). Free circulating T_4 levels are, however, about four to six times that of T_3 and intracellular T_4/T_3 ratios can vary, so it is conceivable that T_4 could occupy a significant fraction of nuclear TRs in some contexts. The lower affinity of T_4 for TRs is probably related to the bulky 5′-iodine moiety that, based on our previous structures of TR-LBDs in complex with T_3 and related agonists, should not fit readily into the hormone binding pocket (14, 16–18). Indeed, placement of some bulky 5′ extensions on high affinity TR agonists can even create antagonists (21). Thus, we asked how T_4 interacts with TR, whether it behaves as an agonist or antagonist, and how it can fit into the TR ligand binding pocket.

TABLE II
Table of neighbor atoms

Distances between the 5′ iodine of T_4 and neighbor atoms, defined as atoms within 4 Å. Hypothetical distances are measured between the T_4 iodine and side chain atoms of the TRβ -T_3 structure, least-squares fitted to the TRβ -T_4 structure in Insight II.

Residue	Real (Å)	Hypothetical	Shift
Met^{310} CE	3.85	3.29	+0.56
Ile^{276} CD1	3.66	3.29	+0.37
Phe^{455} CE1	3.98	3.76	+0.22
Phe^{459} CE1	3.57	3.41	+0.16
His^{435} CE1	3.18	3.08	+0.10
His^{435} NE1	3.23	3.35	−0.12
Met^{313} CE	3.12	3.11	+0.01

We initially examined properties of TR-T_4 complexes. We confirmed that T_4 bound to TR more weakly than T_3, and further demonstrated that T_4 dissociates from TRs faster than T_3, (Fig. 1). Moreover, the TR complex with T_4 is less compact than that with T_3, as suggested by migration of TR-T_4 complexes closer to unliganded TRs than to TR-agonist complexes on HIC (Fig. 2, *A* and *B*) and in gel shift assays with DNA (Fig. 4). The unusual HIC elution profile is not a reflection of lower affinity of TR for T_4, because TR complexes with Dimit (which lacks a 5′ substituent yet only exhibits 20% of the affinity of T_4 for TR) elute at a similar position to TR-T_3 complexes (Fig. 2). It is also unlikely to reflect rapid dissociation of T_4 while on the column, because TRs in complex with radiolabeled T_4 also elute at a similar position to TRs in complex with unlabeled T_4 (Fig. 2*C*). Despite the less compact nature of the TR-T_4 complex, maximally effective doses of T_4 were as effective as those of T_3 in stimulating association of coactivators (GRIP1 and TRAP220; Fig. 3), release of corepressors (N-CoR and SMRT; Fig. 3) and dissociation of TR homodimers from DNA (Fig. 4). Moreover, maximally effective doses of T_4 were as effective as those of T_3 in stimulating activity of a TRE-regulated reporter in cultured cells that express TRα or TRβ, and did so in conditions in which it is unlikely that agonist activity of T_4 stems from contaminating T_3 or intracellular conversion of T_4 to T_3. Thus, it is likely that T_4 and T_3 promote similar overall conformational rearrangements within the TR-LBD in these conditions and that H12 must fold into the active conformation in the presence of T_4.

The crystal structure of the TRβ-T_4 complex supports the notion that T_4 induces a TR conformation similar to that observed with higher affinity agonists (Fig. 6). TR adopts this fold because, overall, T_4 fits tightly into the ligand binding pocket despite the presence of the 5′ iodine group. The pocket accommodates the bulky 5′ iodine via shifts in the position of several amino acid side chains in the pocket relative to their positions in the TR-T_3 complex. These changes enlarge a niche that lies close to the 5′-position of the first thyronine ring and closely matches the size and shape of the 5′ iodine (Figs. 8 and 9). The requirements for these structural alterations for fitting of T_4 relative to T_3 likely explain the reduced affinity of the TRs for T_4 relative to T_3. However, the niche permits H12 to fold over the bulky iodine group and complete the coactivator binding surface. Thus, the presence of an adaptable niche in the TR ligand binding pocket allows T_4 to behave as agonist, despite the 5′-extension.

Although H12 adopts the typical active conformation in the presence of T_4, our crystal structures indicate that the H11-H12 loop is more mobile and more loosely packed against the LBD in the presence of T_4 than in the presence of T_3 (Figs. 6 and 7). These features suggest explanations for the observed differences between the behavior of TR-T_4 and TR-T_3 complexes. A tendency of H12 to oscillate between conformations that resemble liganded and unliganded states would reduce the efficiency of the capping of the pocket and allow T_4 to dissociate more readily. Loose packing of H12 would also expose more of the hydrophobic interior of the protein, explaining unusual mobilities of the TR-T_4 complex in HIC and gel shifts. While T_4 consistently behaves as a full agonist in our hands, it is conceivable that the loose packing of H12 induced by T_4 *versus* T_3 could leave the TR open to external influences that alter the response to the ligand. For example, in cells with high corepressor and/or low coactivator levels, H12 might be forced into the unliganded conformation and T_4 could display partial agonist, or even antagonist, activity. This issue will require further investigation.

We do not yet have a similar structure of TRα in complex with T_4, but there are great overall similarities between the TR isoforms in terms of overall LBD fold (18), sequence and, as reported here, activity in the presence of T_4 and T_3 (Figs. 1, 2, and 5) suggesting that TRα will adapt to the 5′ iodine extension in a similar way to TRβ. Interestingly, T_4 dissociates from TRβ even more rapidly than from TRα (Fig. 1). In this regard, TRβ tends to exhibit less rigidity in the vicinity of the H11-H12 region than equivalent structures of TRα in complex with the same ligand (as judged by temperature factors) (18). These differences in rigidity within the TR H11-H12 region may explain the increased dissociation rate of T_4.

We previously proposed that TR ligands with bulky 5′ side chains should perturb H12 and act as antagonists (reviewed in Ref. 21). This idea, the extension hypothesis (19, 20), has been partly validated by our synthesis of novel TR antagonists based on these principles (22–24), and structures of other NRs in complex with antagonists (such as selective estrogen receptor modulators) (34, 35). Nonetheless, T_4 acts as an agonist, just as we have learned that many other TR ligands with extensions that are even bulkier than the T_4 5′ iodine group can behave as agonists (23, 24). Thus, the nature of the extension and its relationship to the rest of the ligand is important for overall agonist/antagonist activity, and TR must accommodate larger ligands in ways that cannot be easily predicted from structures of TR ligands without "extensions."

NR antagonists perturb H12 position in two ways, by directly interfering with H12 packing or occupying the pocket without inducing the structural changes required for the agonist configuration (reviewed in Ref. 21 and references therein). Our studies add to an emerging pattern, which suggests that NRs alter their conformations in a variety of ways to accommodate hormone analogs and allow them to act as agonists. The TR-T_4 crystal structure reported here reveals that the pocket can reorganize to accommodate the 5′ iodine group, but with a resulting strain of the overall structure relative to T_3. An extreme case of accommodation is for PXR, where the pocket expands to accommodate larger ligands and collapses to accommodate smaller ligands (36–38). In this case, packing does not appear to result in the stability differences we have detected between T_4- *versus* T_3-liganded TRs. Finally, we recently showed that TR accommodates a ligand (GC-24) that binds TRβ with about 40-fold the affinity of TRα, and has a 3′ phenyl extension and a 5′ hydrogen (39), by opening up a hydrophobic patch on the inner surfaces of H3 and H11 that is not normally part of the pocket. It will be interesting to determine how TR accommodates ligands with even bulkier 5′ extensions (22–24), or why ligands with particular 5′ extensions, such as the DIBRT isopropyl group and the NH_3 phenyl group, act as antagonists.

Our studies do not address the question of whether T_4 is a relevant species of TH in physiological settings. As indicated in the Introduction, many factors regulate relative T_4/T_3 concentrations in the nucleus, making it difficult to gauge the extent to which intracellular T_4 participates in TR binding. Nonetheless, the observation that TR can reorganize to create a niche that precisely accommodates the T_4 5′ iodine, coupled with the fact that the potency of T_4 is about 10% that of T_3 in cell culture and that free circulating T_4 concentrations are 4–6-fold those of T_3, raises the distinct possibility that T_4 could exhibit significant agonist activity in humans.

REFERENCES

1. Zhang, J., and Lazar, M. A. (2000) *Annu. Rev. Physiol.* **62,** 439–466
2. Yen, P. M. (2001) *Physiol. Rev.* **81,** 1097–1142
3. Braverman, L. E., and Utiger, R. D. (eds) (2000) *Werner's and Ingbar's The Thyroid: A Fundamental and Clinical Text*, 8th Ed., Lippincott Williams & Wilkins, Philadelphia, PA
4. Kohrle, J. (1999) *Mol. Cell. Endocrinol.* **151,** 103–119
5. Samuels, H. H., Stanley, F., and Casanova, J. (1979) *J. Clin. Investig.* **63,** 1229–1240
6. Apriletti, J. W., Eberhardt, N. L., Latham, K. R., and Baxter, J. D. (1981) *J. Biol. Chem.* **256,** 12094–12101
7. Ichikawa, K., DeGroot, L. J., Refetoff, S., Horwitz, A. L., and Pollak, E. R. (1986) *Metabolism* **35,** 861–868
8. Schueler, P. A., Schwartz, H. L., Strait, K. A., Mariash, C. N., and Oppenheimer, J. H. (1990) *Mol. Endocrinol.* **4,** 227–234
9. Apriletti, J. W., Baxter, J. D., Lau, K. H., and West, B. L. (1995) *Protein Expr. Purif.* **6,** 363–370
10. Surks, M. I., and Oppenheimer, J. H. (1977) *J. Clin. Investig.* **60,** 555–562
11. Silva, J. E., and Larsen, P. R. (1978) *J. Clin. Investig.* **61,** 1247–1259
12. Davis, P. J., Tillmann, H. C., Davis, F. B., and Wehling, M. (2002) *J. Endocrinol. Investig.* **25,** 377–388
13. Weatherman, R. V., Fletterick, R. J., and Scanlan, T. S. (1999) *Annu. Rev. Biochem.* **68,** 559–581
14. Ribeiro, R. C., Apriletti, J. W., Wagner, R. L., Feng, W., Kushner, P. J., Nilsson, S., Scanlan, T. S., West, B. L., Fletterick, R. J., and Baxter, J. D. (1998) *J. Steroid. Biochem. Mol. Biol.* **65,** 133–141
15. Glass, C. K., and Rosenfeld, M. G. (2000) *Genes Dev.* **14,** 121–141
16. Wagner, R. L., Apriletti, J. W., McGrath, M. E., West, B. L., Baxter, J. D., and Fletterick, R. J. (1995) *Nature* **378,** 690–697
17. Darimont, B. D., Wagner, R. L., Apriletti, J. W., Stallcup, M. R., Kushner, P. J., Baxter, J. D., Fletterick, R. J., and Yamamoto, K. R. (1998) *Genes Dev.* **12,** 3343–3356
18. Wagner, R. L., Huber, B. R., Shiau, A. K., Kelly, A., Cunha Lima, S. T., Scanlan, T. S., Apriletti, J. W., Baxter, J. D., West, B. L., and Fletterick, R. J. (2001) *Mol. Endocrinol.* **15,** 398–410
19. Scanlan, T. S., Baxter, J. D., Fletterick, R. J., Kushner, P., Wagner, R., Apriletti, J., West, B., and Shiau, A. (1996) University of California, International Patent
20. Ribeiro, R. C. J., Apriletti, J. W., Wagner, R. L., West, B. L., Feng, W., Huber, R., Kushner, P. J., Nilsson, S., Scanlan, T. S., Fletterick, R. J., Schaufele, F., and Baxter, J. D. (1998) *Recent Prog. Horm. Res.* **53,** 351–394
21. Webb, P., Nguyen, N. H., Chiellini, G., Yoshihara, H. A., Cunha Lima, S. T., Apriletti, J. W., Ribeiro, R. C., Marimuthu, A., West, B. L., Goede, P., Mellstrom, K., Nilsson, S., Kushner, P. J., Fletterick, R. J., Scanlan, T. S., and Baxter, J. D. (2002) *J. Steroid. Biochem. Mol. Biol.* **83,** 59–73
22. Baxter, J. D., Goede, P., Apriletti, J. W., West, B. L., Feng, W., Mellstrom, K., Fletterick, R. J., Wagner, R. L., Kushner, P. J., Ribeiro, R. C. J., Webb, P., Scanlan, T. S., and Nilsson, S. (2002) *Endocrinology* **143,** 517–524
23. Chiellini, G., Nguyen, N. H., Apriletti, J. W., Baxter, J. D., and Scanlan, T. S. (2002) *Bioorg. Med. Chem.* **10,** 333–346
24. Nguyen, N. H., Apriletti, J. W., Cunha Lima, S. T., Webb, P., Baxter, J. D., and Scanlan, T. S. (2002) *J. Med. Chem.* **45,** 3310–3320
25. Swillens, S. (1995) *Mol. Pharmacol.* **47,** 1197–1203
26. Ding, X. F., Anderson, C. M., Ma, H., Hong, H., Uht, R. M., Kushner, P. J., and Stallcup, M. R. (1998) *Mol. Endocrinol.* **12,** 302–313
27. Yuan, C. X., Ito, M., Fondell, J. D., Fu, Z. Y., and Roeder, R. G. (1998) *Proc. Natl. Acad. Sci. U. S. A.* **95,** 7939–7944
28. Hu, X., and Lazar, M. A. (1999) *Nature* **402,** 93–96
29. Ribeiro, R. C., Kushner, P. J., Apriletti, J. W., West, B. L., and Baxter, J. D. (1992) *Mol. Endocrinol.* **6,** 1142–1152
30. Ribeiro, R. C., Apriletti, J. W., Yen, P. M., Chin, W. W., and Baxter, J. D. (1994) *Endocrinology* **135,** 2076–2085
31. Ribeiro, R. C., Feng, W., Wagner, R. L., Costa, C. H., Pereira, A. C., Apriletti, J. W., Fletterick, R. J., and Baxter, J. D. (2001) *J. Biol. Chem.* **276,** 14987–14995
32. Ye, L., Li, Y. L., Mellstrom, K., Mellin, C., Bladh, L. G., Koehler, K., Garg, N., Garcia Collazo, A. M., Litten, C., Husman, B., Persson, K., Ljunggren, J., Grover, G., Sleph, P. G., George, R., and Malm, J. (2003) *J. Med. Chem.* **46,** 1580–1588
33. Nicholls, A., Sharp, K. A., and Honig, B. (1991) *Proteins* **11,** 281–296

34. Shiau, A. K., Barstad, D., Loria, P. M., Cheng, L., Kushner, P. J., Agard, D. A., and Greene, G. L. (1998) *Cell* **95,** 927–937
35. Brzozowski, A. M., Pike, A. C., Dauter, Z., Hubbard, R. E., Bonn, T., Engstrom, O., Ohman, L., Greene, G. L., Gustafsson, J. A., and Carlquist, M. (1997) *Nature* **389,** 753–758
36. Watkins, R. E., Davis-Searles, P. R., Lambert, M. H., and Redinbo, M. R. (2003) *J. Mol. Biol.* **331,** 815–828
37. Watkins, R. E., Maglich, J. M., Moore, L. B., Wisely, G. B., Noble, S. M., Davis-Searles, P. R., Lambert, M. H., Kliewer, S. A., and Redinbo, M. R. (2003) *Biochemistry* **42,** 1430–1438
38. Watkins, R. E., Wisely, G. B., Moore, L. B., Collins, J. L., Lambert, M. H., Williams, S. P., Willson, T. M., Kliewer, S. A., and Redinbo, M. R. (2001) *Science* **292,** 2329–2333
39. Borngraeber, S., Budny, M. J., Chiellini, G., Cunha-Lima, S. T., Togashi, M., Webb, P., Baxter, J. D., Scanlan, T. S., and Fletterick, R. J. (2003) *Proc. Natl. Acad. Sci. U. S. A.* **100,** 15358–15363

Thyroxine-Thyroid Hormone Receptor Interactions

Ben Sandler, Paul Webb, James W. Apriletti, B. Russell Huber, Marie Togashi, Suzana T. Cunha Lima, Sanja Juric, Stefan Nilsson, Richard Wagner, Robert J. Fletterick and John D. Baxter

J. Biol. Chem. 2004, 279:55801-55808.
doi: 10.1074/jbc.M410124200 originally published online October 4, 2004
